

Title: Asymmetric processing of symmetric odour stimuli in the honey bee brain

Authors: Elisa Rigosi^{1,2,3}, Albrecht Haase^{1,2}, Lisa Rath⁴, Gianfranco Anfora³, Giorgio Vallortigara¹, and Paul Szyszka^{4*}

Affiliations:

¹ CIMEC, Center for Mind/Brain Sciences, University of Trento, Corso Bettini 31, 38068 Rovereto (TN), Italy

² Laboratory for Nonlinear Bioimaging, University of Trento, Via delle Regole 101, 38123 Mattarello (TN), Italy

³ Research and Innovation Center, Fondazione Edmund Mach, via E. Mach 1, 38010 San Michele a/A (TN), Italy

⁴ Department of Biology, Neurobiology, University of Konstanz, Universitätsstraße 10, 78457 Konstanz, Germany

* Correspondence to: paul.szyszka@uni-konstanz.de

Abstract: Left-right asymmetries are common properties of nervous systems. Lateralized sensory processing has mainly been described at the behavioural or anatomical level while asymmetric neuronal coding is less studied. Using *in vivo* functional imaging, we identified a left-right asymmetry in the honeybee's primary olfactory centre, the antennal lobe (AL). When odours were symmetrically puffed to the antennae, the neurophysiological distances between odours were higher in the right than in the left AL. Moreover, mixture processing differed between sides: inhibitory interactions occurred mainly in the left, while additive processing occurred mainly in the right AL. Our data suggest a functional specialization between the ALs with the right being tuned for fine odour discrimination. Behavioural data support this hypothesis: bees with amputated right antenna failed in an olfactory foreground-background discrimination task, while bees with amputated left antenna succeeded. The

implementation of different neuronal coding strategies in the left and right brain side may serve to increase coding capacity by parallel processing.

Main Text: If you roll this paper into a cone, fix a visual scene through it with both eyes and then watch it with either the right or the left eye closed, you will experience asymmetric processing of visual stimuli: one eye will probably see a shifted scene. This monocular preference in human binocular vision is thought to avoid binocular functional incompatibility, i.e. conflicting distance information from each eye's images (1). Such avoidance of functional incompatibilities between sensory representations together with the optimization of neural circuitry (avoiding duplication of functions and allowing parallel processing) are thought to be the driving forces in the evolution of left-right asymmetry of sensory systems (2). Although some anatomical and physiological bases of lateralized behaviours are described (3), to our knowledge asymmetric sensory coding has not been studied yet.

The honeybee, *Apis mellifera*, has become an attractive model for investigating olfactory asymmetries at behavioural and sensory levels (4–8). The honeybee olfactory system can process lateralized inputs independently in both sides of the brain (9). There is left-right difference in short-term olfactory memory, favouring the right side (5–8). Moreover, there is a disproportionate distribution in number of sensilla, the olfactory structures on the antenna, with the right antenna showing more sensilla in each segment (4, 7). To date however, evidence of lateralized brain morphology (8) or functions (10, 11) in honey bees is lacking.

Here we tested odour coding in the honey bee brain for left-right asymmetry. Different odours activate different, but often overlapping, ensembles of olfactory receptor neurons (12). From the antenna, olfactory receptor neurons project to the ipsilateral AL. The AL is divided into subcompartments, called glomeruli. Receptor neurons of the same type converge onto the same glomerulus, creating a combinatorial odour code of activated glomeruli (13). We performed *in vivo* calcium imaging of selectively stained output neurons of the glomeruli, the projection neurons (PNs) (14), and compared

odour evoked response patterns in left and right brain sides. Honey bees' antennae were bilaterally stimulated with the single odorants 1-hexanol (H), 2-octanol (O), 1-nonanol (N), and a 1:1 binary mixture (HO) (Fig. 1A). We first compared the background activity, measured as standard deviation before stimulus onset, and found no difference in the fluorescence response ($\Delta F_{340/380}$) between the left and right ALs (left: $0.63 \pm 0.05\%$, right: $0.66 \pm 0.04\%$ (mean \pm SEM)). Odours activated between 20 and 50% of the imaged glomeruli (Fig. 1A, B), and the percentage of activated glomeruli differed between odours but not between sides (Fig. 1B). We then compared the odour response strength (averaged signal during the first second of odour response) between the left and right AL and again, no difference was apparent (Fig. 1C, D). We noted that the global AL response strength to the mixture was larger in the right than in the left AL (Fig. 1C), although there was no significant left-right difference in response strength when the other odours were included in the general RM ANOVA. We then tested whether there is a left-right difference in the processing of mixtures. Each glomerulus' mixture response was compared with its response to the stronger odour component (SO; Fig. 2A). Only in the right AL the response strength for the mixture was stronger than the response strength for the stronger odour component (t-test, $p < 0.001$). This additive mixture processing corresponds to the stronger mixture response observable in the right AL (Fig. 2A). The lack of inhibitory mixture interaction was surprising given its abundance in insect PNs (15–17). We wondered whether the absence of inhibitory mixture interactions might be due to the fact that H and O activate largely overlapping sets of glomeruli (12). Inhibitory mixture interactions in PNs are mainly mediated by lateral inhibition and the effect of lateral inhibition might be masked when the components of a mixture activate the glomerulus equally strong. In contrast, the effect of lateral inhibition might become more prominent with increasing difference between the components. To reveal whether differences in component response strength influence mixture interaction, we separately analysed those glomeruli where the SO was stronger than the weaker odour component (WO, e.g. 3 \times stronger than WO). In the left AL there was a significant mixture

suppression (t-test, $p=0.03$) while there was no mixture interaction in the right AL (Fig. 2A bottom). Mixture interaction indices (MI=mixture-SO) were significantly different between sides (t-test, $p<0.001$). Moreover, we calculated the Pearson's correlation between the mixture interaction index and the difference between components. There was a negative correlation in the left AL and no significant correlation in the right AL. Thus, only in the left AL, mixture suppression increases with increasing difference between the components (Fig. 2B). This side specialization for mixture suppression and additive processing at glomerular level is also visible at the AL level, when the glomerular responses are averaged for each AL, though with less statistical power (Fig. 2C).

We next asked whether there is a qualitative difference in odour representations between the left and right ALs and calculated the Euclidean distances between glomerular response patterns of different odours. The distances between odour evoked glomerular response patterns correlate well with the perceived dissimilarity between them (18). Thus, distances between odour evoked glomerular response patterns contain behaviourally relevant odour information, and left-right differences in inter-odour distances would indicate differences in the discriminatory power of the odour code. Indeed, inter-odour Euclidean distances differed between sides and were higher in the right AL (RM ANOVA, $p<0.05$; Fig. 3A). Bootstrap distributions of Euclidean distances in 10,000 random subsets of data from pooled left and right datasets were calculated to exclude a sampling artefact. Mean values of left and right ALs' Euclidean distances coming from original data fell out the sigma values of their bootstrap distributions for each of the odour pairs (Fig. S1) strengthening the validity of differences which we found in the original samples. To exclude that any difference in the imaged plane between the sides would have systematically affected the population of imaged glomeruli and thus the inter-odour distances, we calculated the Euclidean distances on the basis of identified glomeruli. We measured Euclidean distances between odour response patterns in simulated left-right ALs modelled as vectors built from balanced subsets of identified glomeruli of each side. To this end we calculated Euclidean

distances in 10,000 estimated left-right datasets via bootstrapping method. These Euclidean distances were then compared using a general linear model that revealed a highly significant general difference between sides that was consistent for all odour pairs (Fig. 3B, RM ANOVA, $p < 0.001$). Since we couldn't identify glomeruli in all bees, we additionally calculated the inter-odour distances based on the four most activated glomeruli in all bees. The four most activated glomeruli were mostly located in the central part of the image view. Therefore, they should always be visible, even in case of a possible left-right difference in the image planes. This analysis confirmed the higher distances between odour representations in the right AL (Fig. S2, RM ANOVA, $p < 0.05$).

Finally, in order to better visualize the difference in odour distances along time in the two ALs, we performed a principle component analysis (PCA) and projected the odour-induced responses of all 426 left and 455 right glomeruli into a 2 dimensional space (represented by the two first principle components which capture 77% and 79% of the variability in the left and right ALs, respectively). Interestingly, odour-evoked trajectories in PCA spaces were similar in the two sides but the relative distances between inter-odour patterns were larger across glomeruli in the right ALs (Fig. 3C).

There is good evidence that PNs' activity patterns indeed encode odour identity and underlie odour perception (18, 19). Accordingly, the higher neurophysiological odour distances in the right AL might support perceptual odour discrimination. To test this hypothesis we trained bees with single antenna in use (the other one being amputated) to extend their proboscis when a foreground odour was presented over a different background odour. Only bees that were able to perceptually separate the foreground and background odours would be able to learn this task. Bees with only their right antenna in use succeeded while bees with only their left antenna in use did not (Fig. 4A, RM ANOVA, $p < 0.01$). The right antenna dominance on this task was not due to a better discrimination for changes in odour concentrations: when both groups of bees were trained to discriminate an increased concentration of the background odour, they failed equally (Fig. 4B). We finally tested whether the different abilities in

odour discrimination were driven by a side difference in the performance during discriminatory learning. Bees with either the right or the left antenna in use performed equally during differential conditioning (Fig. 4C). Thus, odour coding in the right brain sides might support bees' ability to perceive two odours as different rather than learning to discriminate between them.

Functional compartmentalization of different tasks in the left and right side are well known in a variety of animal species (2, 20). Here we showed that a bilateral odour stimulus is qualitatively differentially encoded in the left and right brain sides and that this asymmetric odour code is consistent with asymmetric behavioural performance. To date, there are a few studies showing lateralized neuronal responses to sensory stimuli (21–24) but to our knowledge lateralization has never demonstrated at the level of a neuronal population code.

Our results contradict conclusions from previous calcium imaging studies that found symmetric odour response patterns in the honey bee ALs (10, 11). However, both studies imaged ALs using bath staining technique, which is not selective for a particular neuron type and probably mostly reflects activity in olfactory receptor neurons (25). Therefore, the left-right difference which we found might be due to left-right difference in processing within the AL network rather than left-right difference in glomerular pattern of receptor neuron activity.

Our results are consistent with previous studies that revealed anatomical and behavioural lateralization in bees (4–6, 26). Recently, Rogers and colleagues (27) showed a right dominance for context-dependent behaviours, in particular during tasks that implicates nestmate recognition. It is possible that this behavioural specialization might reflect a higher olfactory discriminative power with the right antenna that has been shown here. What is the advantage of lateralized odour coding? The olfactory system constantly performs two seemingly opposing tasks: discriminating between odorants, concentrations and mixture compounds on the one hand and generalizing across them on the other hand. These opposing tasks require opposing coding strategies. To fulfil these opposing coding

strategies, the olfactory system may utilize parallel processing which is a common feature both in the insect AL (28) and in the mammalian olfactory bulb (29). The left-right asymmetry in odour coding which we found here might reflect another mechanism of functional compartmentalization that allows the simultaneous use of different coding schemes and therefore increases the computational capacity of the olfactory system, without any structural compartmentalization to be imposed.

References and Notes:

1. G. Kommerell, C. Schmitt, M. Kromeier, M. Bach, Ocular prevalence versus ocular dominance. *Vision Res.* **43**, 1397–1403 (2003).
2. L. J. Rogers, G. Vallortigara, R. J. Andrew, *Divided Brains The Biology and Behaviour of Brain Asymmetries* (Cambridge Univ. Press, 2013).
3. M. L. Concha, I. H. Bianco, S. W. Wilson, Encoding asymmetry within neural circuits. *Nat. Rev. Neurosci.* **13**, 832–843 (2012).
4. P. Letzkus *et al.*, Lateralization of olfaction in the honeybee *Apis mellifera*. *Curr. Biol.* **16**, 1471–6 (2006).
5. L. J. Rogers, G. Vallortigara, From antenna to antenna: lateral shift of olfactory memory recall by honeybees. *PloS ONE* **3**, e2340 (2008).
6. G. Anfora, E. Frasnelli, B. Maccagnani, L. J. Rogers, G. Vallortigara, Behavioural and electrophysiological lateralization in a social (*Apis mellifera*) but not in a non-social (*Osmia cornuta*) species of bee. *Behav. Brain Res.* **206**, 236–9 (2010).

7. E. Frasnelli, G. Anfora, F. Trona, F. Tassarolo, G. Vallortigara, Morpho-functional asymmetry of the olfactory receptors of the honeybee (*Apis mellifera*). *Behav. Brain Res.* **209**, 221–5 (2010).
8. E. Rigosi *et al.*, Searching for anatomical correlates of olfactory lateralization in the honeybee antennal lobes: a morphological and behavioural study. *Behav. Brain Res.* **221**, 290–4 (2011).
9. J. C. Sandoz, R. Menzel, Side-specificity of olfactory learning in the honeybee: generalization between odors and sides. *Learn. Mem.* **8**, 286–94 (2001).
10. C. G. Galizia, K. Nägler, B. Hölldobler, R. Menzel, Odour coding is bilaterally symmetrical in the antennal lobes of honeybees (*Apis mellifera*). *Eur. J. Neurosci.* **10**, 2964–2974 (1998).
11. J. C. Sandoz, C. G. Galizia, R. Menzel, Side-specific olfactory conditioning leads to more specific odor representation between sides but not within sides in the honeybee antennal lobes. *Neuroscience* **120**, 1137–1148 (2003).
12. C. Galizia, R. Menzel, The role of glomeruli in the neural representation of odours: results from optical recording studies. *J. Insect Physiol.* **47**, 115–130 (2001).
13. C. G. Galizia, P. Szyszka, Olfactory coding in the insect brain: molecular receptive ranges, spatial and temporal coding. *Entomol. Exp. Appl.* **128**, 81–92 (2008).
14. S. Sachse, C. G. Galizia, Role of inhibition for temporal and spatial odor representation in olfactory output neurons: a calcium imaging study. *J. Neurophysiol.* **87**, 1106–17 (2002).
15. N. Deisig, M. Giurfa, J. C. Sandoz, Antennal lobe processing increases separability of odor mixture representations in the honeybee. *J. Neurophysiol.* **103**, 2185–94 (2010).

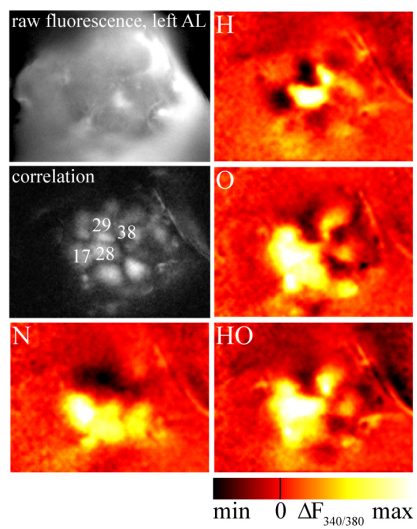
16. J. S. Stierle, C. G. Galizia, P. Szyszka, Millisecond stimulus onset-asynchrony enhances information about components in an odor mixture. *J. Neurosci.* **33**, 6060–9 (2013).
17. A. F. Silbering, C. G. Galizia, Processing of odor mixtures in the *Drosophila* antennal lobe reveals both global inhibition and glomerulus-specific interactions. *J. Neurosci.* **27**, 11966–77 (2007).
18. F. Guerrieri, M. Schubert, J. C. Sandoz, M. Giurfa, Perceptual and neural olfactory similarity in honeybees. *PLoS Biol.* **3**, e60 (2005).
19. P. Szyszka *et al.*, Mind the gap: olfactory trace conditioning in honeybees. *J. Neurosci.* **31**, 7229–39 (2011).
20. E. Frasnelli, G. Vallortigara, L. J. Rogers, Left-right asymmetries of behaviour and nervous system in invertebrates. *Neurosci. Biobehav. Rev.*, 1–19 (2012).
21. J. W. Peirce, K. M. Kendrick, Functional asymmetry in sheep temporal cortex. *Neuroreport* **13**, 2395–9 (2002).
22. J. S. Kanwal, Right-left asymmetry in the cortical processing of sounds for social communication vs. navigation in mustached bats. *Eur. J. Neurosci.* **35**, 257–70 (2012).
23. A. Poremba *et al.*, Species-specific calls evoke asymmetric activity in the monkey 's temporal poles. *Nature* **427**, 448–451 (2004).
24. M. A. Pinsk, K. DeSimone, T. Moore, C. G. Gross, S. Kastner, Representations of faces and body parts in macaque temporal cortex: a functional MRI study. *Proc. Natl. Acad. Sci. U. S. A.* **102**, 6996–7001 (2005).

25. C. G. Galizia, R. Vetter, in *Advances in Insect Sensory Neuroscience*, T. A. Christensen, Ed. (CRC press, Boca Raton, 2004), pp. 349–392.
26. S. Biswas *et al.*, Sensory regulation of Neuroligins and Neurexin I in the honeybee brain. *PLoS ONE* **5**, e9133 (2010).
27. L. J. Rogers, E. Rigosi, E. Frasnelli, G. Vallortigara, A right antenna for social behaviour in honeybees. *Sci. Rep.* **3**, 2045 (2013).
28. W. Rössler, M. F. Brill, Parallel processing in the honeybee olfactory pathway: structure, function, and evolution. *J. Comp. Physiol. A* (2013).
29. K. M. Igarashi *et al.*, Parallel mitral and tufted cell pathways route distinct odor information to different targets in the olfactory cortex. *J. Neurosci.* **32**, 7970–85 (2012).
30. L. Rath, C. Giovanni Galizia, P. Szyszka, Multiple memory traces after associative learning in the honey bee antennal lobe. *Eur. J. Neurosci.* **34**, 352–60 (2011).

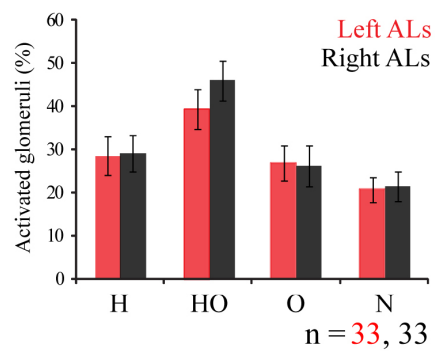
Acknowledgements

Thanks to C. Giovanni Galizia, Christoph Kleineidam and Jacob Stierle for fruitful discussion, Andrew J Anderson, Nicholas Kirkerud, and Martin Strauch for statistical advice, and Teresa Bluhmki, Mihaela Coric, Michael Lutz, and Sina Rometsch for help with the behavioural experiments. This study was supported by *Provincia Autonoma di Trento* and the *Fondazione Cassa di Risparmio di Trento e Rovereto* (to ER, AH, GA, GV), *Provincia Autonoma di Trento* (Project IBRAIM to AH) and Bundesministerium für Bildung und Forschung (01GQ0931 to PS).

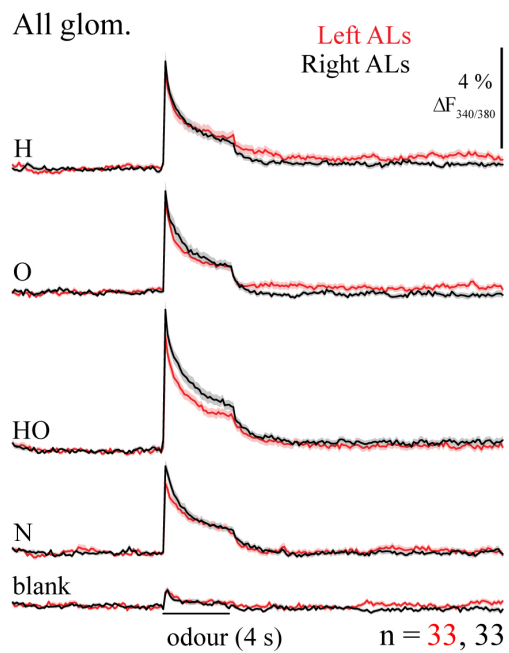
A



B



C



D

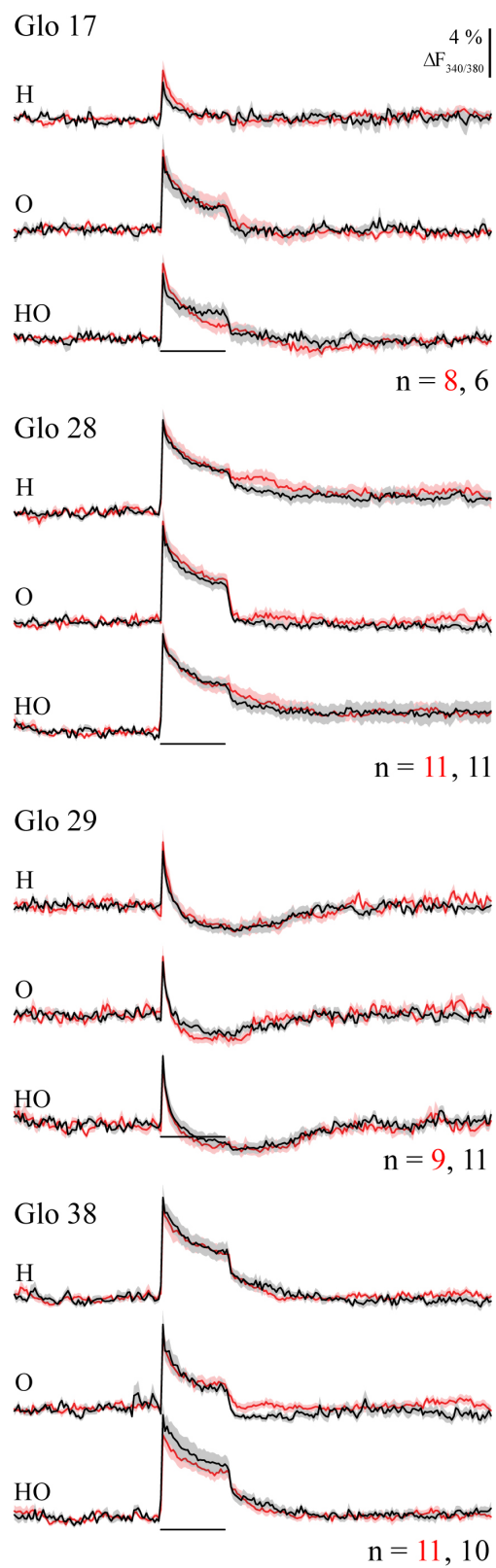


Fig. 1. PN response strength does not differ between sides. (A) Calcium imaging in PNs (raw fluorescence, left AL), correlation image of the same AL (correlation) with identified glomeruli whose odour responses is represented in D and colour coded images showing odour evoked glomerular activity to 2-nonanol (N), 1-hexanol (H), 2-octanol (O), and a 1:1 mixture of 1-hexanol and 2-octanol (HO). (B) The number of odour-activated glomeruli is equal between sides. Percentage of activated glomeruli for different odour stimuli: each glomerulus was considered active when activity during the first second of odour response showed a signal $\geq 6 \times \text{SD}$ before stimulus onset. For each bee the percentage of activated glomeruli was calculated as mean \pm SEM for left and right ALs ($N=33$ per side). The percentage of activated glomeruli differed between odours ($F(3,192)=23.436$, $p<0.001$) but not between sides ($F(1,64)=0.143$, $p=0.706$) and there was no interaction between side and type of odorant (odour \times side $F(3,192)=0.706$, $p=0.529$). (C) Time-course of global PN responses to odours along the whole recordings (29s) (average over all glomeruli; mean \pm SEM); Grey bars indicate the 4 s stimulus pulse. The RM ANOVA revealed an odour effect ($F(3,192)=25.57$, $p<0.001$) but neither side effect (side $F(1,64)=2.59$; $p=0.112$) nor interactions (odour \times side $F(3,19)=1.390$; $p=0.25$) were found. (D) Time-course of PN responses to odours in identified glomeruli averaged across animals.

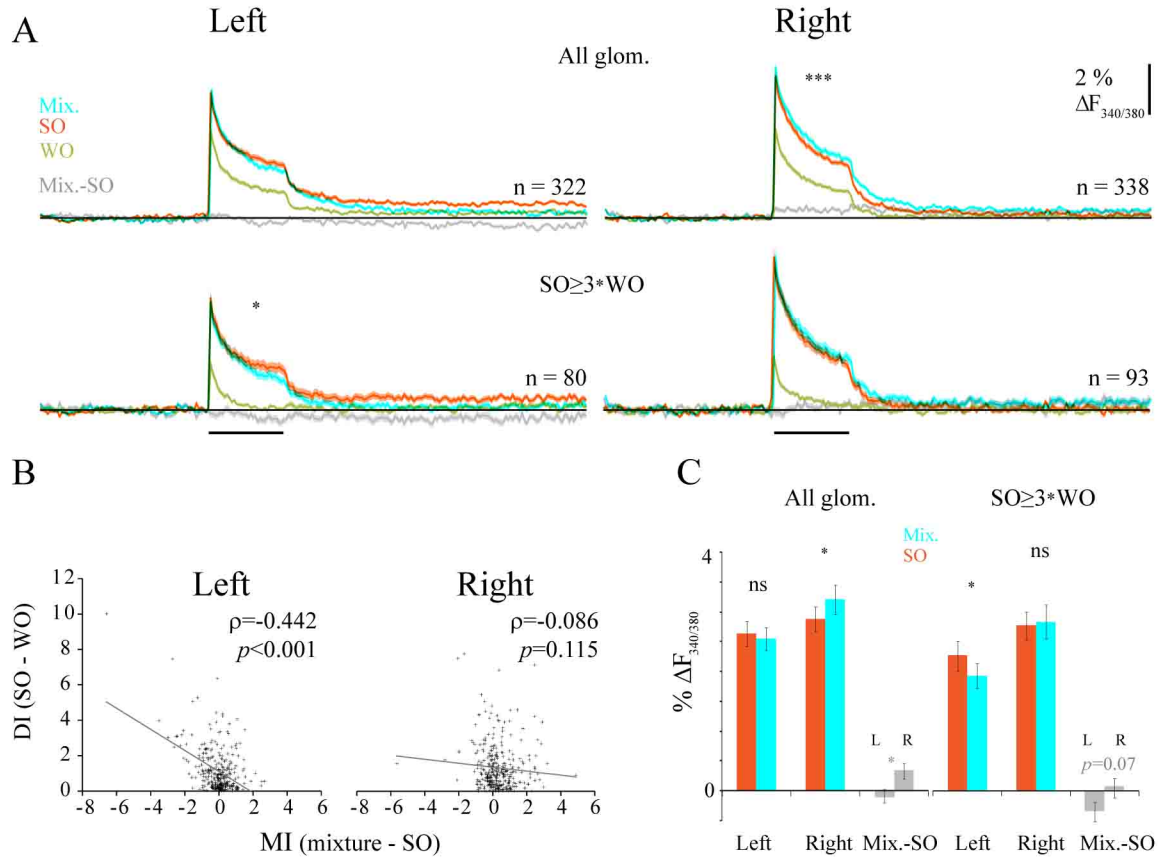
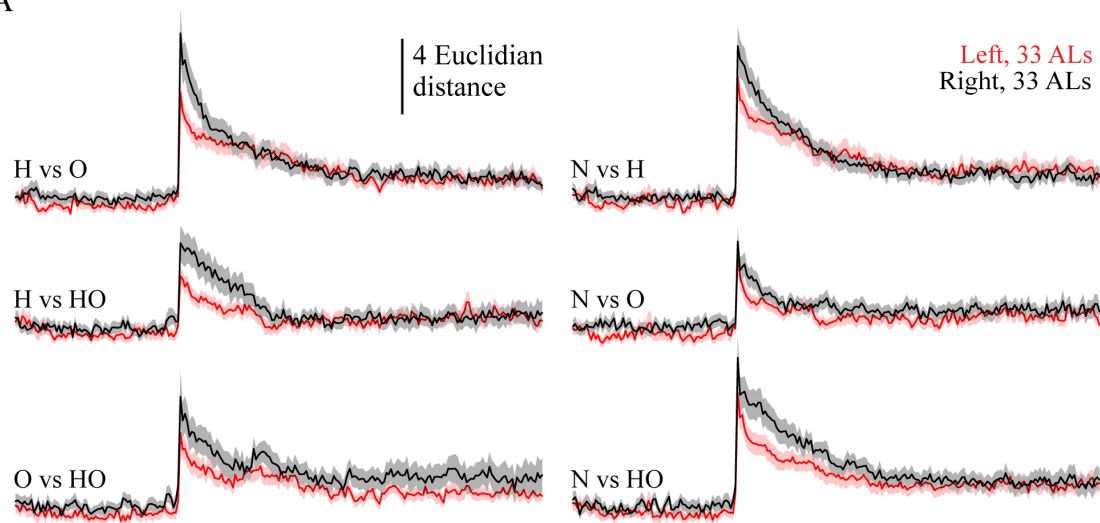


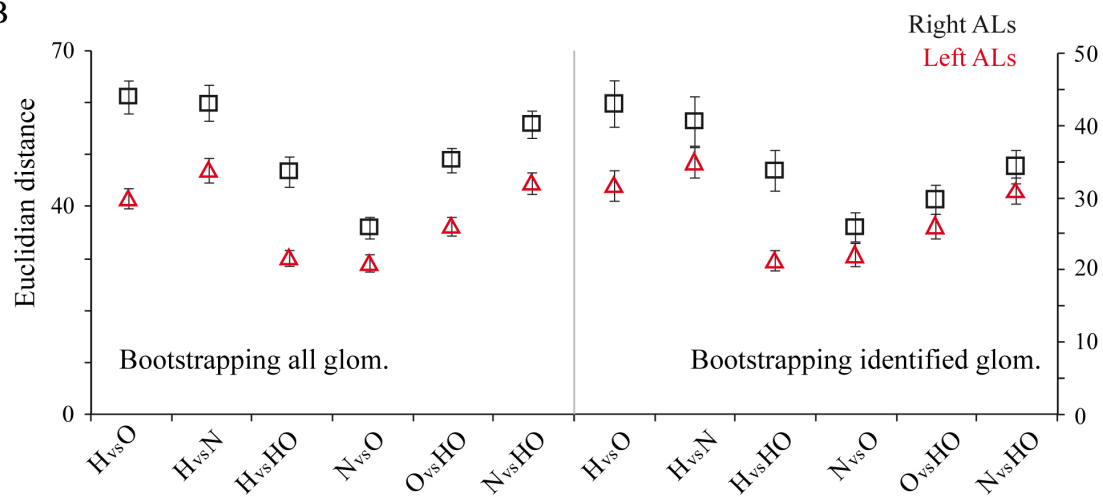
Fig. 2. Mixture processing differs between the left and right AL. (A) Top: Time course of PN activity (mean \pm SEM) in glomeruli which responded positively to both components, in the left and right ALs. Different colours represent responses to the mixture (cyan); stronger odour (SO) (orange), weaker odour (WO) (green) and the difference between Mix-SO (grey). **Bottom:** Same as above, but only those glomeruli where $SO \geq 3 \times WO$ were considered. **(B)** Dot plots show the response strength differences between mixture components (DI) versus the response strength differences between mixture and SO for all glomeruli with positive responses (left AL: 322 glomeruli; right AL: 338 glomeruli). Only in the left AL there is a negative correlation between the two ($\rho = -0.442$, $p < 0.001$, Pearson correlation), showing that inhibitory mixture interactions increase with increasing response strength difference between SO and WO. In the Left AL the correlation between two indices was significantly stronger than in the right AL (Z-transformation test, $z = -4.97$; $p < 0.001$). **(C)** Left and right

AL differ in sign and degree of mixture effects. Averaged SO (orange bars) and mixture (cyan bars) responses in each AL calculated only for glomeruli with positive responses to both mixture components (left panel) and or those glomeruli where $SO \geq 3 \times WO$ (average \pm SEM, $N=33$ ALs per side). Grey bars show the averaged MI. Grey asterisks indicate differences between sides in the interaction indices. L: left ALs, R: right ALs. (*: $p < 0.05$; ***: $p < 0.001$, 'ns': not significant).

A



B



C

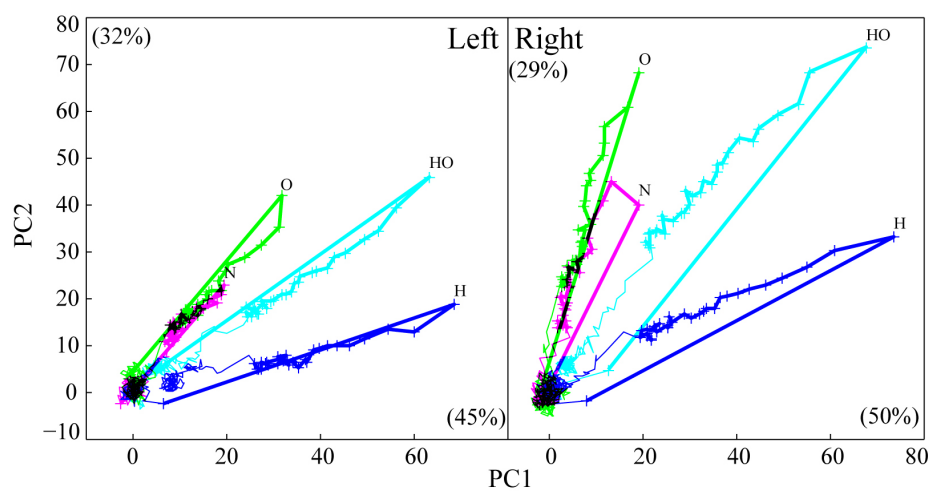


Fig. 3. Distances between odour response patterns are greater in the right AL. (A) Time course of Euclidean distances for each odour pair (average over all bees; mean \pm SEM) in left (red) and right (black) ALs. The bar indicates the 4s stimulus pulse. (B) **Left graph:** Euclidean distances (mean \pm SD) measured in left and right AL created in 10,000 simulated antennal lobes made by combinations of all glomeruli datasets. Euclidean distances means are calculated over the first second of odour stimuli. **Right graph:** Same as left graph but for identified glomeruli only. (C) Trajectories of the odour responses in all glomeruli of left ALs (426 glomeruli) and right ALs (455 glomeruli) calculated using PCA. Bold lines indicate the 4 s odour stimulation. Crosses represent the time points of sampled frames during odour stimulation (125 ms inter frame interval). Percentage of variability explained by PC1 and PC2 is given in brackets. H: 1-hexanol; O: 2-octanol; N: 2-nonanol; HO: 1:1 mixture of 1-hexanol and 2-octanol.

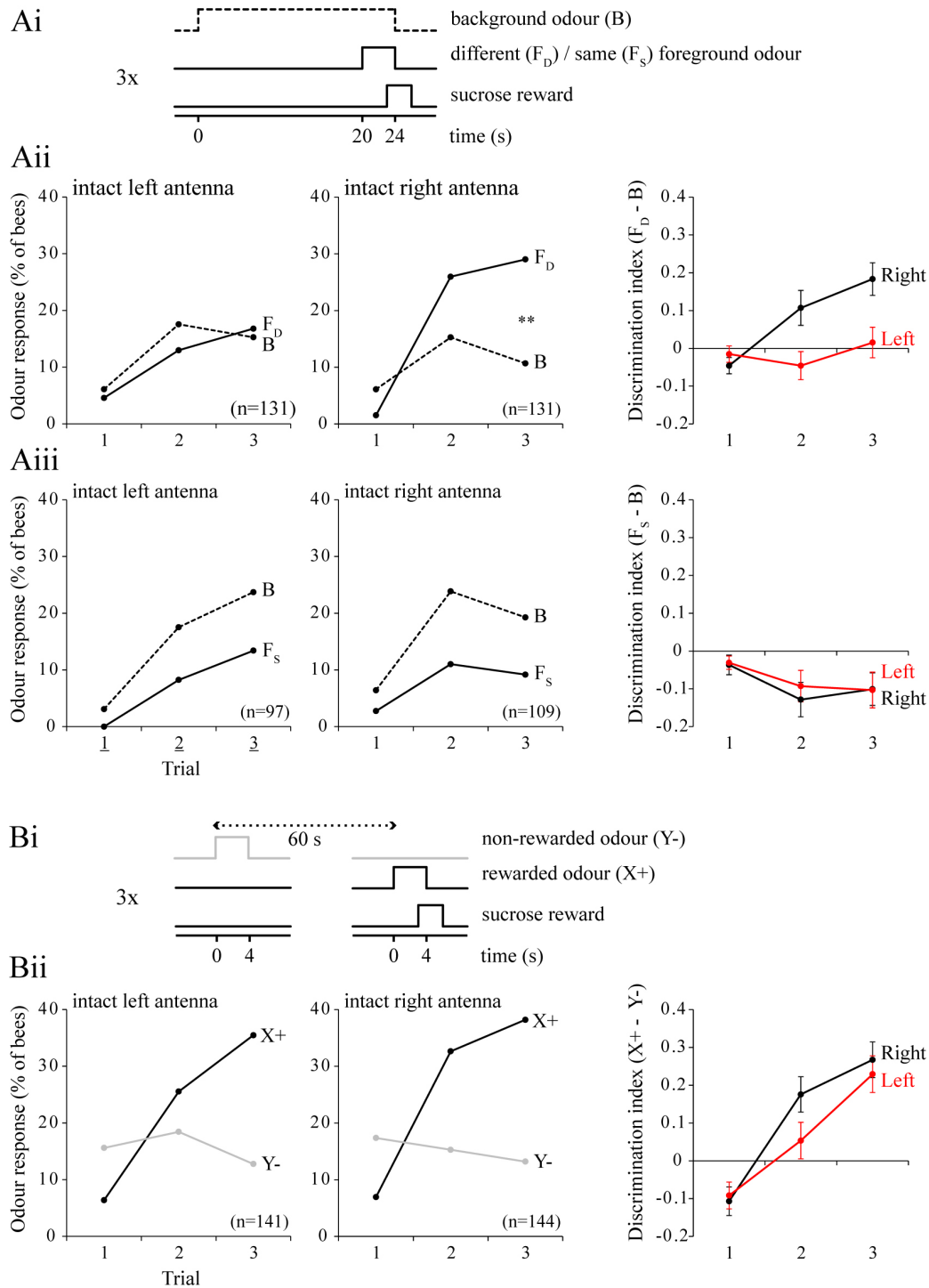


Fig. 4. Bees with amputated right antenna fail in an olfactory foreground-background discrimination task. (Ai) Timing of background odour, foreground odour and sucrose reward during the learning experiment. The background odour started 20 seconds before the onset of foreground

odour, and the sucrose reward started 3 seconds after the onset of the foreground odour. Bees received three conditioning trials. Inter-trial intervals was 60 seconds. **(Aii)** Bees were trained to discriminate a foreground odour F_D from a different background odour B. Behavioral performance during conditioning was measured as proboscis extension response to the initial 3 seconds of the odour stimuli. The discrimination index is the response difference between F_D and B (average over bees, \pm SEM). **(Aiii)** same as in aii) but the foreground odour F_S was the same as the background odour. **(Bi)** Bees were differentially conditioned to discriminate between a rewarded odour X+ and a non-rewarded odour Y-. Bees underwent a 3 \times pseudo-randomized presentations of X+ and Y- (inter-trial interval: 60 s). Odours were delivered for 4 s, sugar solution was presented for 3s (1 s overlap with X+). **(Bii)** Behavioural responses over the 3 conditioning trials and discrimination index were calculated as in aii.

Supplementary Materials:

Material and Methods

Calcium imaging data came from published data and unpublished data from the same experiment (30). The recordings were performed on either the left or the right AL. In total, 66 bees were imaged, 33 left ALs and 33 right ALs. Details of the method can be found elsewhere (30). Briefly, animal preparation and imaging experiments were performed with honey bee foragers. PNs of both ALs were stained with the calcium sensitive dye Fura-2 dextran (Invitrogen). The next day, bees were prepared for imaging and the AL that showed better staining and spontaneous activity was brought into focus.

PNs in the AL were imaged with a water immersion objective (20x, NA 0.95, Olympus) with a wide-field imaging system (Till Photonics) and a CCD camera (Imago QE, Till Photonics). 8 \times 8 pixels of the camera were binned on-chip resulting in a resolution of 172 \times 130 pixels. Each recording lasted 29 s and

consisted of 232 double frames recorded with 340 and 380 nm excitation light, respectively, at a frame rate of 8 Hz. Excitation and emission light was separated with a 420 nm dichroic mirror and a 490-530 nm emission filter. Bees were stimulated with 1:100 dilutions of 1-hexanol, 2-octanol, 1-nonanol, a mixture of 1-hexanol and 2-octanol, and the solvent mineral oil as blank control (all from Sigma Aldrich). For all the experiments odours were prepared daily from stocks in mineral oil, which were renewed every 4 weeks. Odour stimuli were delivered as 4 s pulses with a custom-built computer controlled olfactometer (19). Each channel of the olfactometer consisted of two syringes, an empty one for equalizing air flow and one containing the odorant. The olfactometer had 6 channels. The air stream through each channel was 300 ml/min, each controlled by a flow meter (Analyt-MTC). Odours were injected into a continuous carrier air stream (1200 ml/min) in a glass tube (1 cm in diameter), which was directed to the bee positioned 1 cm in front of it. A solenoid three ways valve (Lee) controlled the odour pulses by diverting air from the empty syringe to the odorant syringe. The six channels added up to 1800 ml/min, and total air stream was 3000 ml/min. Continuous air suction behind the bee cleared residual odour. Odours were presented in a pseudo-randomized order with an inter-trial interval of 2 min.

Data analysis

Imaging data were analysed using custom-written programs in IDL (RSI). Movies were movement corrected by aligning frames within and between measurements. Glomeruli were segmented with help of an unsharp masked image of the raw fluorescence and a correlation image where the correlation of the signal traces between neighbouring pixels was calculated. The ratio of the images acquired at 340 and 380 nm excitation wavelength was calculated and the average background fluorescence was subtracted from every frame of a measurement to get the fluorescence response signal $\Delta F_{340/380}$. The

background fluorescence was calculated as mean of 66 frames (frames 4-69) before stimulation. No filtering was used for quantitative analysis.

Response strength was quantified as the mean signal during 1 s after stimulus onset (frames 72-79). To calculate the global response over the whole AL, for each bee, the response of each glomerulus was calculated and averaged over all glomeruli. Spontaneous activity was calculated as standard deviation (SD) before stimulus onset (frames 1-70) averaged over all glomeruli. Left and right spontaneous activities were compared with an independent t-test (two tails).

Glomeruli whose activity during the first second of odour response showed a signal $\geq 6 \times \text{SD}$ before stimulus were considered as active. Numbers of activated glomeruli were compared at the level of the AL (averaged per bee) using a repeated measures analysis of variance (RM ANOVA) with odours as within-subject factor and side as a between-subjects factor.

For evaluating differences in mixture interactions between sides the stronger odour component (SO) was determined for each glomerulus, showing the strongest response to one of the two components of the mixture (i.e. it is the minimum response to mixture if no inhibitory interaction would occur with the mixture (17)). All glomeruli which showed a positive signal during odour activation (frames 72-103) were considered. For each AL the SO and the mixture were compared across glomeruli (paired t-test, two-tails). An interaction index ($\text{MI} = \text{mixture} - \text{SO}$) was calculated and right and left indices were compared using an independent t-test (two tails). An index of response strength difference between the components of the mixture in each antennal lobe ($\text{DI} = \text{SO} - \text{WO}$) was calculated and Pearson correlation analysis was performed between the two indices in each AL. Coefficients of the left and right ALs were compared using Fisher's z-transformation test. Finally, those glomeruli that showed $\text{SO} \geq 3 \times \text{WO}$ were selected. The SO and mixture responses were compared within each glomerulus in the two ALs (paired t-test, two tails) as well as the interaction indices between left and right antennal lobes (independent t-test, two tails).

In order to analyse mixture interactions at the level of the whole AL, glomerular responses were averaged within each individual and SO and mixture responses were compared for each side separately (paired t-test, two tails) as well as interaction indices between sides (independent t-test, two tails).

The distance between odour response patterns was quantified as follows: for each AL, the response of each glomerulus was calculated and the odour response pattern was represented as a vector in the glomerular response space. Distances between two odour responses were quantified by calculating the Euclidean distance between the two vectors as follows:

$$d_{ij} = \sqrt{\sum_{k=1}^p (X_{ki} - X_{kj})^2}$$

With i and j indicating two odours; p the number of glomeruli; X_{ki} the activity of glomerulus k when stimulated with odour i .

Odour distances were analysed separately using RM ANOVA with distances as a within-subject factor and side as a between-subjects factor.

A principal component analysis (PCA) was performed for left and right antennal lobes separately (using the Matlab princomp function). For each odour, the PCA was applied to the multi-dimensional glomerular space (426 glomeruli for the Left AL; 455 for the right AL) for the whole recording period (29s) (16).

For measuring consistency of side differences, Euclidean distances were calculated in a bootstrapping simulation based on 10,000 subsets in which AL data from the 66 bees was randomly divided into two groups (33 ALs each group). In a second simulation, only data from identified glomeruli was considered. 10,000 datasets were created, where left and right glomerular data was randomly sampled with a balanced number of data points for each glomerulus type. Euclidean distances were calculated between odours for the glomerular vectors of these groups. Results in the left and right groups were

compared using RM ANOVA with distances as a within-subject factor and side as a between-subjects factor.

Quantitative and statistical analyses were performed using Matlab (R2012b, Mathworks) and PASW Statistic 18 (SPSS).

Behavioural experiments

Honey bee foragers were collected from outdoors hives between March and June 2013 in Konstanz (Germany). They were individually mounted in plastic holders as described elsewhere (19), allowing for free movement of antennae and mouth parts. Bees were fed until satiation with 1M sugar solution. The next day experiments were performed. Before starting the odour conditioning, honey bees were randomly divided into two groups, in one group the right antenna was cut at the base of the pedicel, in the second group the left antenna was cut; antennae were cut 15 to 60 minutes before the experiment.. Each bee was put in front of a custom-built olfactometer (see above) and an exhaust fan removed the odour quickly after exposure.

Bees received three conditioning trials during which an odour (conditioned stimulus, CS) was presented for 4 s paired with 1 M sugar reward (unconditioned stimulus, US), which was presented for 3 s, 1 s CS-US stimuli overlap. The inter-trial intervals were 1 min in all behavioural experiments. In each conditioning session 8 bees with amputated left antenna and 8 bees with amputated right antenna were conditioned in parallel.

During the odour segregation task (Fig. 4A, B) the CS was a foreground odour (F_D , number of bees with only left antenna in use (N_L)=131; number of bees with only the right antenna in use (N_R)=131; F_S , N_L =97, N_R =107) that was superimposed on a different or the same background odour (B) (delivered

from 20 s before the exposure of F_D or F_S). Background and foregrounds odours were equally often 1-hexanol and 2-octanol (both 1:100 v/v in mineral oil).

In a differential conditioning protocol (Fig. 4C, $N_L=141$, $N_R=144$), a rewarded odour ($X+$) and a non-rewarded odour ($Y-$) were presented in a pseudo-randomized order (either $X+, Y-, Y-, X+, Y-, X+$ or $Y-, X+, X+, Y-, X+, Y-$; X and Y were either 1-hexanol or 2-octanol, both 1:100 v/v in mineral oil). Behavioural data were analysed with RM ANOVA with trials and odour stimuli as a within-subject factor and side as a between-subjects factor.

Supplementary Figures

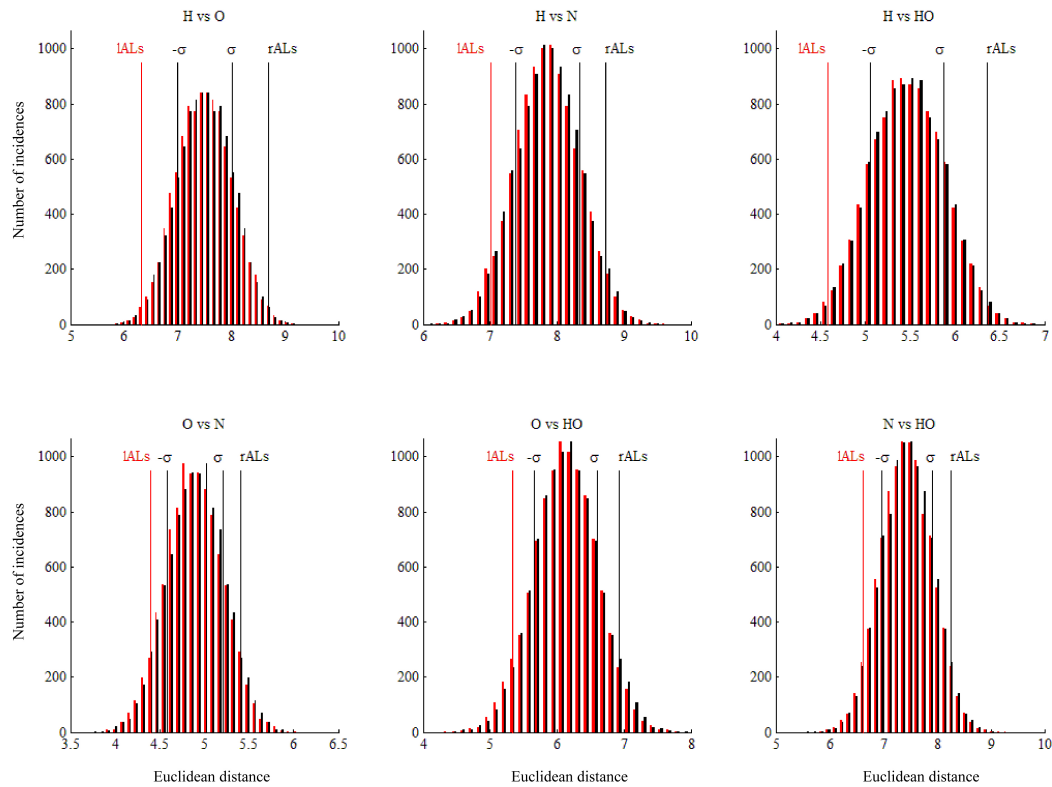


Fig. S1 The difference in the Euclidean distances between the left and right ALs is not caused by sampling artefacts. Histograms show Euclidean distances calculated in 10,000 sets, where the joined data of left and right ALs ($N=66$ bees) were randomly divided into two subgroups of $N=33$ bees each (red and black bars) and sorted into 30 bins. The Euclidean distances obtained from original left and right ALs fell beyond the standard deviation σ of the resampled distributions, which are perfectly overlapping. The resampled distributions are shown for each odour pairs, H: 1-hexanol; O: 2-octanol; N: 2-nonanol; HO: 1:1 2-octanol: 1-hexanol mixture. *X* axis: Bins of Euclidian distance values calculated within each AL (from the average response during the first second of odour stimulation). *Y* axis: Number of incidences within the distribution s in the two resampled subgroups (black and red bars). Grey lines mark the $\pm\sigma$ values of the resampled distributions. Original left and right AL Euclidean distances are marked with red and black lines, respectively.

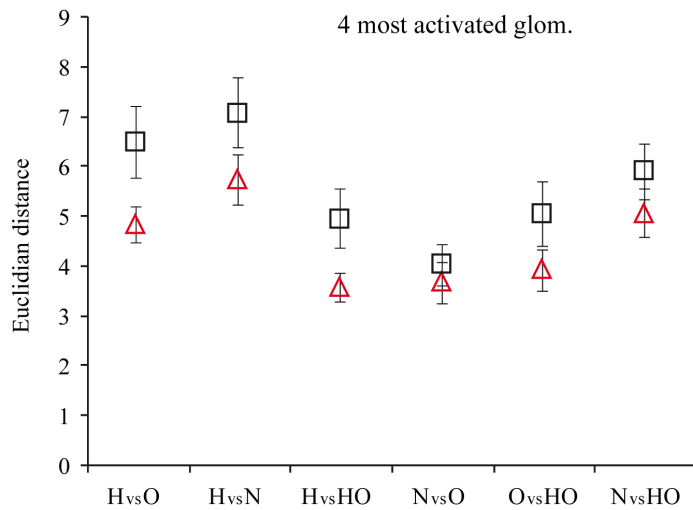


Fig. S2 Euclidean distances in left (red triangles) and right (black squares) ALs calculated using the 4 most activated glomeruli only. Mean \pm SEM are shown for each odour pair (*X* axis). A general side effect is still present, analysing only this subset of data (RM ANOVA, $p<0.05$).